## 9

#### **Wood Physics/Mechanical Properties**

Honghai Liu\*, Jiajia Wang and Na Huang

# Moisture response characteristics of the rheological behavior of heat-treated North American alder wood during the moisture absorption process

https://doi.org/10.1515/hf-2025-0022 Received March 18, 2025; accepted September 1, 2025; published online September 23, 2025

Abstract: The temperature and relative humidity (RH) have an impact on the moisture absorption rate, moisture distribution, and swelling behavior of wood, which can lead to wood absorptive rheological phenomena such as swelling stress and swelling strain. This study examined the absorption and rheological characteristics of heat-treated (HT) and conventionally kiln-dried (CKD) North American alder wood under different conditions (50, 70, and 90 °C at 90 % RH) from an absolutely dry state to target moisture content (MC) levels (5 %, 10 %, and 15 %). The results showed that heat treatment significantly reduced the moisture absorption rate, the difference in MC, and the radial swelling ratio of the wood, with maximum reductions of 0.94-points, 1.54-points, and 0.89points, respectively. The differential swelling between wood's surface and core generates stresses and swelling strains ( $\varepsilon_E$ ,  $\varepsilon_V$ ,  $\varepsilon_M$ ). These stresses showed a trend opposite to that of the drying stress. Heat treatment notably reduced the mechano-sorptive swelling creep strain (MSCS) in North American alder wood (47.3 % lower at 70 °C and 0.7 % lower at 90 °C). In contrast, there were no significant differences in free swelling strain, elastic swelling strain, and viscoelastic swelling creep strain between HT and CKD wood.

**Keywords:** heat-treated wood; moisture absorption; swelling ratio; rheological properties

**Jiajia Wang and Na Huang**, College of Furnishings and Industrial Design, Nanjing Forestry University, Nanjing, 210037, China. https://orcid.org/0009-0007-3739-4129 (J. Wang)

#### 1 Introduction

Wood is a natural material with porous, hygroscopic, and anisotropic properties (Lyu et al. 2023; Xu et al. 2022a, b; Fan et al. 2014; Feng and Zhao 2011). While its biodegradability and environmental benefits make it widely applicable (Huang et al. 2024; Yue et al. 2016; Liu et al. 2021). However, the free hydroxyl groups in the chemical components of wood are highly hygroscopic. When wood is exposed to the air, changes in ambient temperature and humidity can affect its shrinking, wetting, and deformation, leading to internal stress (He et al. 2019; Yang and Liu 2020; Zhong et al. 2021). This reduces the dimensional stability and mechanical strength of the wood, thus limiting its further use in precision engineering and high-humidity environments (Ermeydan et al. 2021; Xu et al. 2022a, b; Yang et al. 2019; Zhu and Yang 2025). Therefore, reducing moisture content (MC), increasing dimensional stability, and reducing stress are crucial for the widespread application of wood.

Heat treatment has emerged as an environmentallyfriendly physical modification method to tackle these problems. By reducing the equilibrium moisture content and minimizing dimensional variations, heat treatment significantly enhances the stability of wood (Yang and Jin 2021; Zhang et al. 2021; Ding et al. 2015; Feng et al. 2022). However, in industrial applications, there is often a requirement for conventionally heat-treated (HT) wood, such as that modified at 180–220 °C under inert gas, superheated steam at atmospheric pressure, or in vacuum conditions, to quickly absorb and regain moisture to reach specific moisture content (MC) levels for further processing. This process is the opposite of drying. When the wood absorbs moisture under harsh conditions such as high temperature and high humidity, a significant MC gradient will form between the surface and the core zones of the wood. This can lead to asynchronous swelling of the surface and core layers, thereby generating absorptive stress. This phenomenon is similar to drying stress but occurs during the moisture

<sup>\*</sup>Corresponding author: Honghai Liu, Jiangsu Co-Innovation Center of Efficient Processing and Utilization of Forest Resources, Nanjing Forestry University, Nanjing, 210037, China; and College of Furnishings and Industrial Design, Nanjing Forestry University, Nanjing, 210037, China, E-mail: liuhonghai2020@njfu.edu.cn

absorption process (Yang and Liu 2021; Yang et al. 2022). If these stresses are not properly managed, they may cause warping, cracking, or even structural failure in the finished wood products.

Numerous previous studies on the moisture absorption of HT wood have been conducted under standard ambient conditions of 25 °C and 60 % relative humidity (RH), across the full humidity range from 0 to 95 % RH. These studies mainly focused on the dimensional stability of HT wood after moisture absorption (Li et al. 2008; Zhou et al. 2006; Militz and Altgen 2014; Jiang and Lyu 2012; Jiang et al. 2023). For example, Schneider and Rusche (1973) showed that vacuumheated beech (Fagus silvatica L.) and spruce (Picea asperata Mast) had reduced moisture absorption. Kocaefe et al. (2015) investigated the dimensional stability of different wood species after heat treatment at 180-200 °C. The swelling ratio of these treated woods was significantly lower than that of other species, with a remarkable decrease in swelling ranging from 50 to 80 %.

There have been few studies on HT North American alder wood (Alnus rubra Bong.), such as the one by Lazarescu et al. (2014). However, these studies mainly focused on moisture absorption at room temperature, ignoring the dynamic stress evolution and rheological behavior during moisture absorption at elevated temperatures. This research gap is crucial because harsh conditions such as high temperature and high humidity can shorten the moisture absorption time of HT wood. Nevertheless, they will induce moisture absorption stress and strain in the wood, which affects the dimensional stability and subsequent processing performance of the wood. Patcharawijit et al. (2018) have shown that humidity significantly influences the mechanosorptive creep of Chinese fir (Cunninghamia lanceolata) during the moisture absorption process. Fu et al. (2016) also emphasized that drying defects in wood are typically related to drying stress, and they measured the tangential and radial drying strains in birch (Betula platyphylla). However, they did not conduct a more in-depth analysis of how the variations in stress magnitude and direction across different layers contribute to the overall differences in mechanical response.

In this study, the absorption rate, MC distribution, tangential and radial swelling ratios, and rheological properties of HT and conventionally kiln-dried (CKD) North American alder wood were investigated to systematically examine the effects of absorption conditions on the absorption rate behavior and the development of stress and strain. The findings provide a theoretical and practical basis for moisture absorption protocols and the control of stress and strain in HT wood.

#### 2 Materials and methods

#### 2.1 Materials

The test material consisted of North American alder boards with dimensions of 20 mm (radial, R)  $\times$  70 mm (tangential, T)  $\times$  4,000 mm (longitudinal, L) supplied by Mage Company in Chongqing, China. Nine boards were selected and dried at 80 °C and 65 % RH using the CKD method until their MC reached 10 %. Subsequently, the wood was longitudinally bisected, and the right-hand portion was HT at 160 °C for 6 h under superheated steam conditions. After that, endmatched defect-free specimens measuring 20 mm (R)  $\times$  70 mm  $(T) \times 600 \,\mathrm{mm}$  (L) were cut from the CKD and HT boards respectively, which were from the same original boards. In total, there were 27 HT (group H) boards with an initial MC of 8.0 % and 27 CKD (group C) boards with an initial MC of 10.0 %.

#### 2.2 Moisture absorption tests

Three moisture absorption tests were conducted at a RH of 90 % and temperatures of 50 °C, 70 °C, and 90 °C respectively. Figure 1 is a schematic diagram of the sample preparation process for the test at 50 °C and 90 % RH. Nine CKD boards were selected and divided into three C groups (CA<sub>1-3</sub>, CB<sub>1-3</sub>, and  $CC_{1-3}$ ), with three specimens in each group. Meanwhile, the corresponding nine HT boards were divided into three H groups (HA<sub>1-3</sub>, HB<sub>1-3</sub>, and HC<sub>1-3</sub>) (Figure 1a). Prior to the test, all boards were dried in an oven (Model DHG-9503BS-III, Shanghai Xinmiao Medical Equipment Manufacturing Co., Ltd) at 103 °C until they reached an absolutely dry state. Subsequently, they were marked in red at the center of the boards, and both ends of the boards were sealed with epoxy resin adhesive. After that, the dimensions of the absolutely dry boards in the tangential and radial directions were measured using vernier calipers (Model CD-20CPX, with an accuracy of 0.01 mm, Mitutoyo, Japan). The absolutely dry mass of the boards was measured using an electronic balance (Model JA5003N, with an accuracy of 0.001 g, Shanghai Precision Scientific Instrument Co., Ltd). Finally, all the boards were placed in a constant temperature and humidity chamber (Model DF-Hs-408, Nanjing Defu Experimental Equipment Co., Ltd) set at 50 °C and 90 % RH for moisture absorption.

During the moisture absorption process, each board was taken out at certain time intervals to measure its dimensions and mass so as to obtain its MC and dimensions. When each board in Group 1 reached the target MC of 5%, it was

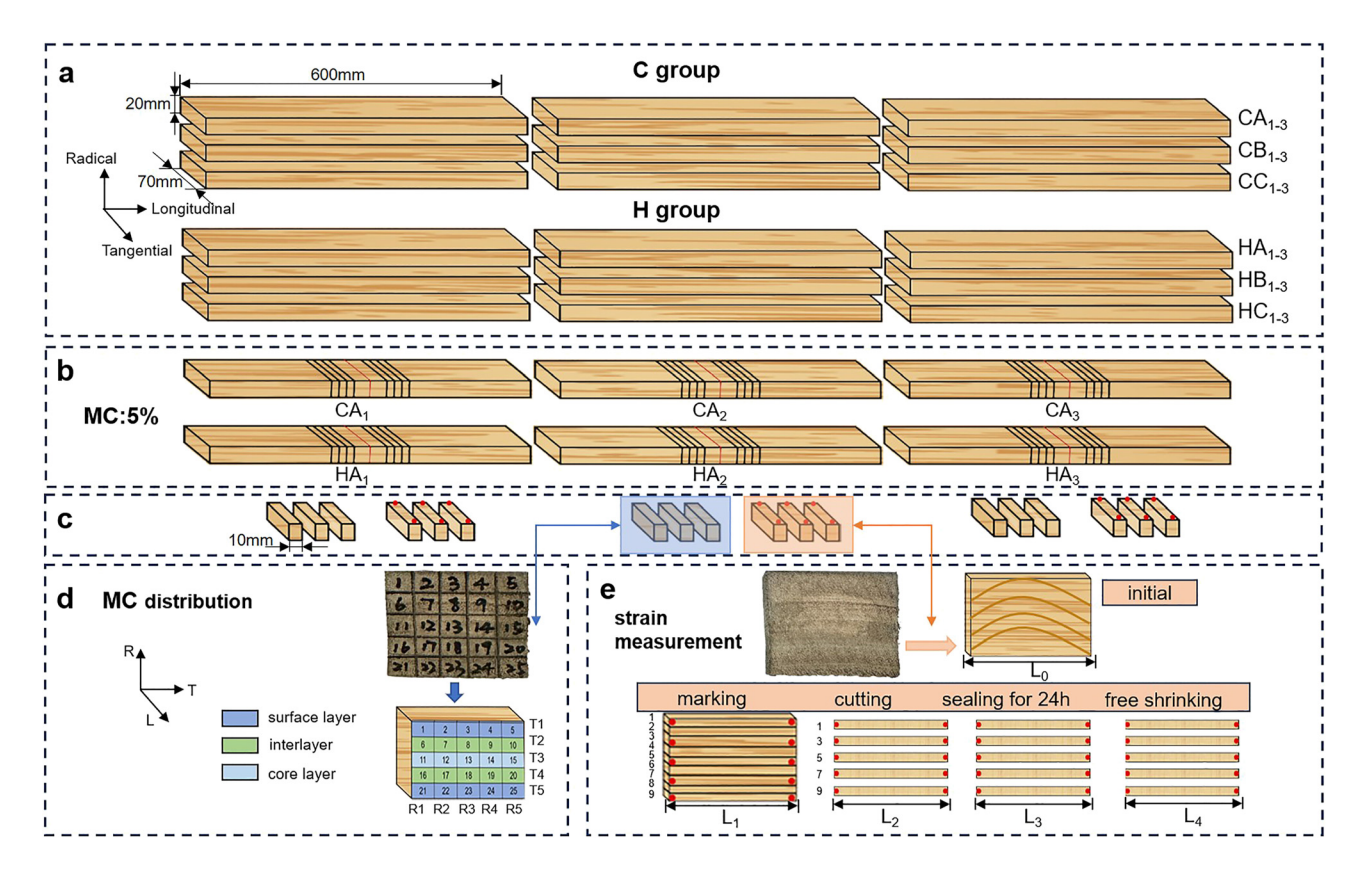


Figure 1: Schematic diagram of test sample preparation.

removed from the chamber and then marked for the measurement of MC distribution, dimensions, and strain (Figure 1b).

As shown in Figure 1c, each board was first sawn in the middle. From the left-hand part of the board, three endmatched wood slices with dimensions of 20 mm (R) × 70 mm  $(T) \times 10 \text{ mm}$  (L) were sawn for MC determination. From the right-hand part of the board, three end-matched wood slices of the same dimensions were sawn for strain measurement. For the slices used for MC determination, they were numbered and then dissected into 25 wood blocks as soon as possible (Figure 1d), and then placed into a Ziploc bag. The blocks were removed from the Ziploc bag one by one for mass measurement, and then they were dried in an oven at 103 °C to obtain the absolute dry mass. For the slices used for strain measurement, they were labeled along the tangential direction and marked with dots at the ends, and then split into nine strips along the tangential direction. The strips with odd numbers were quickly placed into a Ziploc bag. Then, one strip was removed from the Ziploc bag, and the distance between the two dots of the strip was measured using scanning images and ImageJ software at four stages: after sawing  $(l_1)$ , after splitting  $(l_2)$ , after the dimensions became stable  $(l_3)$ , and after free swelling  $(l_4)$  (Figure 1e).

When the MC of Group 2 and Group 3 reached 10 % and 15 % respectively, the same operations were carried out. It was noteworthy that the values measured here represented the state of the samples after a short handling period after they were removed. Although this error may cause slight variations in the absolute values of MC, swelling ratio, and strain, both groups underwent the same handling procedures. This ensured that any such error affected them equally.

# 2.3 Determination of moisture content and absorption rate

Moisture content was determined based on the absolute dry mass of the wood, following the GB/T1927.4-2021 "Part 4: Determination of moisture content" standard. The moisture absorption rate (MAr) was calculated using formula (1) based on the change in MC between two measurement points and the time interval between them.

MAr = 
$$\frac{M_1 - M_0}{t} \times 100 \%$$
 (1)

where  $M_0$  represents the MC at the previous measurement point, %;  $M_1$  represents the MC at the measurement point

after absorption, %; and t is the time interval between the two measurement points.

#### 2.4 Determination of swelling ratio

The tangential and radial dimensions of the boards in the absolute dry state, as well as during the process of moisture absorption, were measured using vernier calipers. The swelling ratio in the tangential and radial directions of the specimen was calculated using formula (2) in accordance with the GB/T1927.8-2021 "Part 8: Determination of Wet Expansion" standard.

$$S = \frac{l - l_0}{l_0} \times 100 \% \tag{2}$$

where S is the tangential or radial swelling ratio of the boards, %, l is the tangential or radial dimension of the boards after absorbing, mm, and  $l_0$  is the tangential or radial dimension of the specimen in the absolute dry state, mm.

#### 2.5 Measurement of rheological properties

With the incorporation of wood rheology theory into wood drying, the total strain under drying stress is divided into free shrinkage strain, elastic strain, viscoelastic creep strain, and mechano-sorptive creep strain (MSCS) (Rice and Youngs 1990; Chávez et al. 2021). In contrast, when dry wood is exposed to wet conditions, stress could occur because the swelling in the wood surface and core zones is not synchronized during the absorption process. In this study, this stress is referred to as absorptive stress. Consequently, the absorptive stress during wood absorption gives rise to a total absorptive swelling strain, which consists of free swelling strain ( $\varepsilon_S$ ), elastic swelling strain ( $\varepsilon_E$ ), viscoelastic swelling creep strain ( $\varepsilon_V$ ), and mechano-sorptive swelling creep strain ( $\varepsilon_M$ ). These strains correspond to those during wood drying. The free swelling strain is reversible with moisture adsorption and occurs without mechanical stress. The elastic swelling strain is fully recoverable upon unloading and results from the immediate deformation of the cell wall under applied stress. The viscoelastic swelling creep strain is a time-dependent and partially recoverable deformation that occurs under constant load and MC. The mechano-sorptive swelling creep strain is the additional, irreversible creep specifically induced by the change in MC under load.

Before moisture absorption, the surfaces of the boards were marked with dots. Then, the boards were placed into the scanner (CanoScan700F, 48-bit color, Canon China Co. Ltd.) to measure the initial distance  $l_0$  (in the absolute dry

state) between the measurement points. When each board reached the target MC, strain slices were sawn from the right-hand part in the middle of the boards and labeled along the tangential direction. Dots were marked at the ends of the slices (Figure 1e). At this time, the distance ( $l_1$ ) between the two points was measured (Figure 2). Next, the strain slices were split into strips along the tangential direction. After the odd-numbered strips were fixed with special tools, the distance  $(l_2)$  between the points on these strips was measured. After that, the strips were put into a resealable bag with the air removed. Once the dimensions of the strips became stable, the distance  $(l_3)$  between the points on the strips was measured. Finally, the strips were immersed in distilled water for 24 h, steamed for 8 h to restore any plastic deformation, and then conditioned at the corresponding temperature and RH of the absorption process until their MC increased to 5 %, 10 %, and 15 % respectively. Then, the distance  $(l_4)$  between the points on the strips was obtained. The various strains of the specimen were calculated according to formulae (3), (4), (5), and (6).

$$\varepsilon_{S} = \frac{l_1 - l_0}{l_0} \tag{3}$$

$$\varepsilon_E = \frac{l_2 - l_1}{l_0} \tag{4}$$

$$\varepsilon_V = \frac{l_3 - l_2}{l_0} \tag{5}$$

$$\varepsilon_M = \frac{l_4 - l_3}{l_0} \tag{6}$$

where  $l_0$  is the distance between measurement points on the surfaces of absolutely dry boards, mm;  $l_1$  is the distance between the two end points in the strain slices after sawing, when the boards have absorbed moisture up to the target MC, mm;  $l_2$  denotes the distance between the two end points in the strips after splitting the strain slices, mm;  $l_3$  is the distance between the two end points in the strips after they have reached dimensional stability, mm; and  $l_4$  represents the distance between the two end points in the strips after the strips have freely swelling to the target MC, mm.

### 3 Results and analysis

#### 3.1 Moisture absorption rate

Figure 3a illustrates the variation in MC over time for groups H and C at temperatures of 50, 70, and 90  $^{\circ}$ C. Figure 3b shows the average moisture absorption rates for these groups when they reach target MC of 5 %, 10 %, and 15 % at the same



Figure 2: Diagram of strain measurement of the specimen by ImageJ.

temperature. For both group H and C, the MC exhibited nearly linear increases at 90 °C, while at 50 °C, the increase was more gradual. The maximum MC of group H and C at 90 °C was 13.03 % and 15.38 %, respectively. Under all three temperature conditions, the moisture absorption rate increased notably with rising temperature and decreased as the wood's MC increases for both groups H and C. Notably, group H had a slightly lower moisture absorption rate compared to group C, the analysis indicated that there was a statistically significant difference between Group H and Group C (P < 0.05). In the early stages of moisture absorption, the difference in absorption rates between the two groups was small at 70 and 90 °C, but this difference became more pronounced at 50 °C throughout the entire process. The average differences

between group H and C at 50, 70 and 90 °C was 0.94 %-points, 0.35 %-points, 0.83 %-points per hour, the heat treatment was most pronounced at 50 °C. A multifactor ANOVA was conducted on the absorption rates of groups H and C at the three temperatures (Table 1). The results indicated that temperature significantly affected the moisture absorption rate for both groups, with group H exhibiting lower moisture absorption than group C. This finding aligned with theoretical studies suggesting that heat treatment effectively reduces wood's moisture absorption (Hill et al. 2021).

#### 3.2 Moisture content distribution

Figure 4 illustrates the distribution of MC in the T1 to T5 layered strips of Group H and Group C at various temperatures under target moisture conditions of 5 %, 10 %, and 15 %. The MC in the T1 to T5 layered strips exhibited a symmetrical distribution along the radial direction of the wood. During the moisture absorption process from 0 % to 15 %, the MC of the surface layered strips (T1 and T5) in both Group H and Group C was higher than that of the sub-layered strips (T2 and T4), with the core layered strips (T3) having the lowest MC. At all three temperatures, the MC of each layered strip in Group H was significantly lower than that in Group C, except for the conditions at 50 °C and a target MC of 5 %. The

**Table 1:** Results of multifactor ANOVA for absorption rates of Group H and Group C wood at temperatures of 50 °C, 70 °C, and 90 °C.

Source	Degrees of freedom	Mean square	F	Significance <i>P</i> -value
Groups	1	0.98	2.01	0.16
Temperature	2	7.33	14.97	0.00
$Group \times temperature$	2	0.31	0.64	0.53

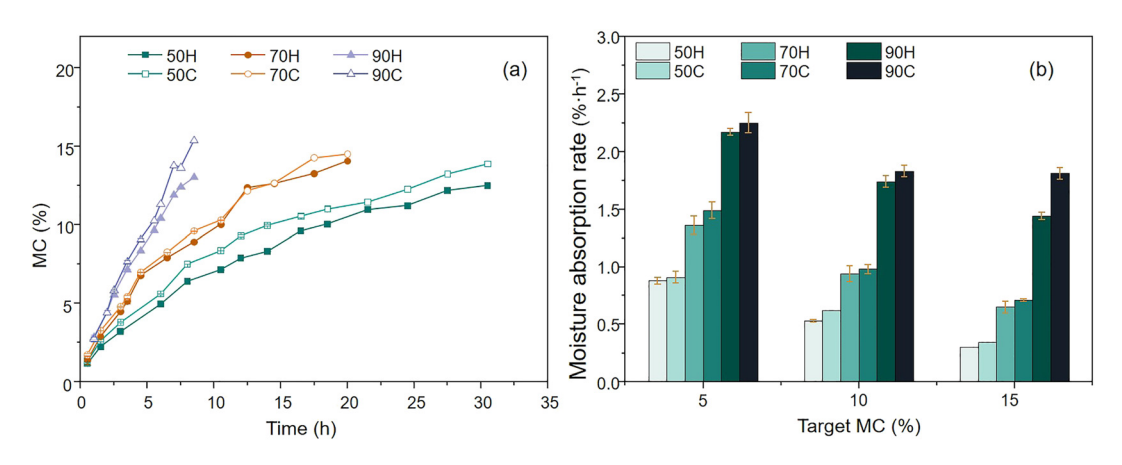


**Figure 3:** Change curves of moisture content (a) and comparison of average moisture absorption rate (b) of Group H and Group C wood at temperatures of 50 °C, 70 °C, and 90 °C.

analysis indicated that there was a significant difference in MC levels between Group H and Group C (P < 0.05). This indicated that heat treatment had an inhibitory effect on moisture absorption. The varying MC levels in the T1 to T5 layered strips during moisture absorption resulted in different degrees of swelling, leading to internal stress between the layered strips.

The MC differences between the surface and core layers of Group H and Group C are shown in Table 2. At 70 and 90 °C, for both groups, the MC difference decreased as the MC of the wood increased. However, at 50 °C, the difference was greatest when the MC reached 10 % (H group: 2.90 %-points, C group: 2.63 %-points). This was attributed to the slower absorption rate at lower temperatures. Generally, the MC difference between the surface and core layers of Group H was smaller than that of Group C, indicating that heat treatment effectively reduced this difference. This reduction in MC variability diminishes the stress caused by the MC difference and, consequently, the resulting strain.

#### 3.3 Swelling ratio

The swelling ratio in the tangential and radial direction during moisture absorption process is shown in Figure 5. The

swelling ratio in the T and R direction of the group H and group C under the three conditions increased with the increase of MC, and the swelling ratio in the T direction was greater than that in the R direction at the end of moisture absorption. The analysis indicated that there was a significant difference between Group H and Group C (P < 0.05). The swelling ratio of H group was significantly lower than that of C group during the absorption process, especially in the R direction. The greatest differences in T and R direction between groups H and C occurred at 90 °C, presenting increase with temperature. This indicates that heat treatment has an inhibitory effect on the rate of swelling, help reducing the swelling of H groups and resulting lower internal stress and strain (Gao 2016; Yin et al. 2023), the reduction in swelling coefficients exceeds reported values for ring-porous hardwoods like oak (Kubovský et al. 2020). Meanwhile, at the same MC, the swelling ratio in T and R directions for both group H and group C increased with temperature increasing, indicating temperature is a critical factor for wood swelling.

The parameters of the linear fitting equations for the swelling ratio and MC of Groups H and C are presented in Table 3. The results showed that both tangential and radial swelling ratios exhibited a clear linear relationship with MC for both groups. The slope, representing the swelling coefficient, was generally smaller for Group H compared to

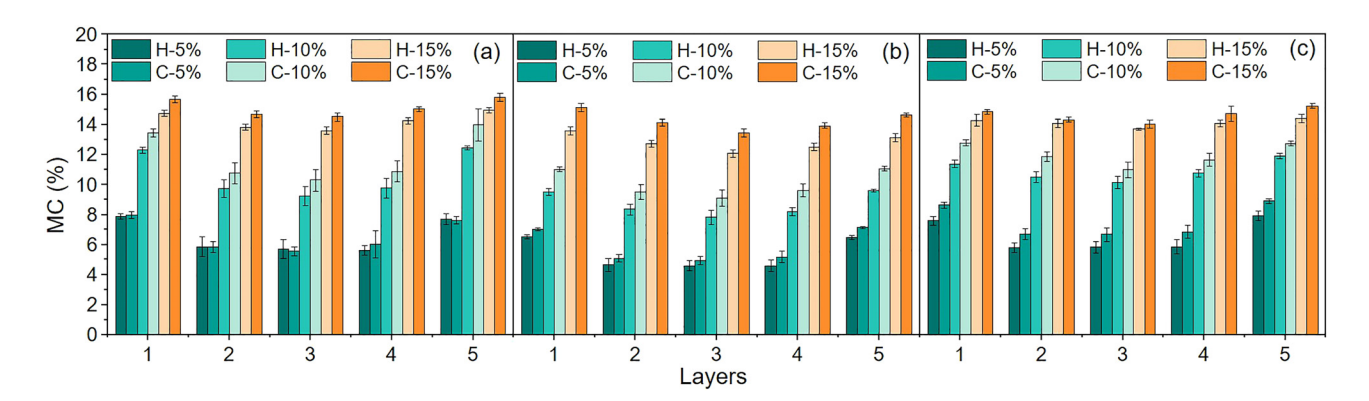


**Figure 4:** Distribution of moisture content in the T1 to T5 layered strips of Group H and Group C wood under target MC of 5 %, 10 %, and 15 % at temperatures of (a) 50 °C, (b) 70 °C and (c) 90 °C.

Table 2: The difference in MC (%) between the surface layer and core layer of Group H and Group C wood at temperatures of 50 °C, 70 °C, and 90 °C.

Temperature (°C)	50				70		90			
Target MC (%)	5	10	15	5	10	15	5	10	15	
Group C	1.88 ± 0.10	2.90 ± 0.15	0.88 ± 0.08	1.87 ± 0.12	1.48 ± 0.11	0.85 ± 0.08	2.01 ± 0.09	1.00 ± 0.01	0.52 ± 0.05	
Group H	$2.06 \pm 0.18$	$2.63 \pm 0.12$	$0.79 \pm 0.07$	$1.88 \pm 0.10$	$1.27 \pm 0.10$	$0.75 \pm 0.06$	$1.94 \pm 0.08$	$1.00 \pm 0.07$	$0.27 \pm 0.03$	

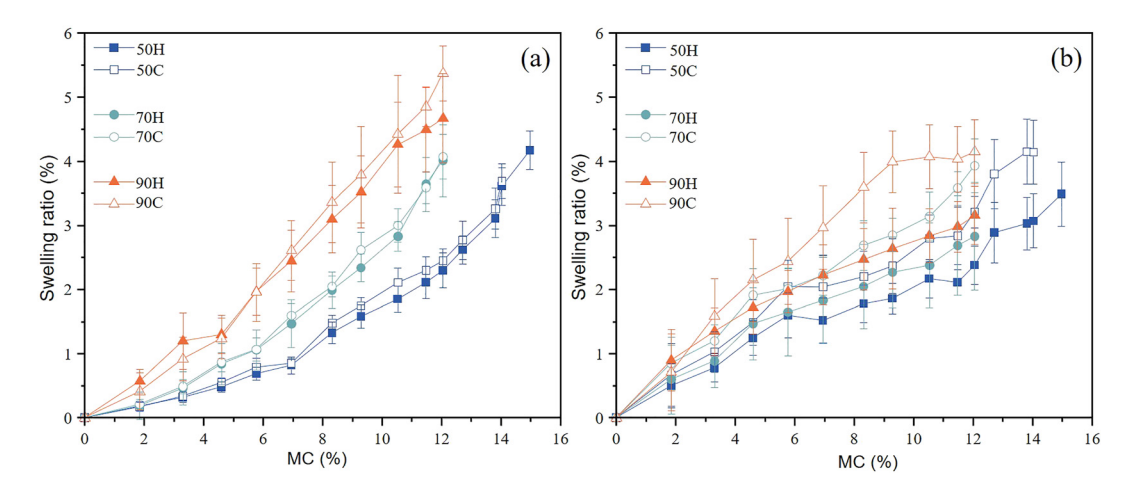


**Figure 5:** The swelling ratio during moisture absorption process in the tangential direction (a) and in the radial direction (b) of Group H and Group C wood at temperatures of 50 °C, 70 °C, and 90 °C.

Group C, particularly in the radial direction. This indicated that heat treatment reduced the North American alder wood's swelling capacity, resulting in less swelling and lower internal stress.

#### 3.4 Rheological property

During the process of moisture absorption from an ovendried state to targeted MC, no significant differences were observed in free swelling strain, elastic swelling strain, or viscoelastic swelling creep strain between Groups H and C. However, a statistically significant difference was observed in MSCS between the two groups (P < 0.05).

Figure 6a illustrates that as MC increased, the free swelling strain in both groups increased. Multifactorial analysis of variance indicated that temperature had no significant impact on free swelling strain. At MC of 5 %, 10 %, and 15 %, the maximum free swelling strains were 0.0072, 0.0293, and 0.0474, respectively.

Due to differing moisture absorption rates between internal and external wood regions, uneven moisture distribution occurs. This triggers asynchronous swelling

phenomena, leading to stress and strain changes (Gao 2016). Figure 6b shows symmetric distributions of elastic swelling strain in the surface layers and interlayers of H group and C group. Stress patterns for both groups followed similar trends, with compressive stress occurring in the surface layer and tensile stress developing in the interlayers and core layer, though slightly stronger strain was observed under 90 °C conditions. Surface layers exhibited compressive stress because their faster moisture absorption caused swelling, which was constrained by adjacent inner wood. At 50 °C and 90 °C, compressive stress increased with MC, peaking at a value of -0.0039 for HT wood at 90 °C. Conversely, interlayers and core layers exhibited tensile stress, which decreased with increasing MC and reversed to compressive stress at 50 °C and 90 °C. Notably, heat treatment did not significantly affect elastic swelling strain, as no differences were observed between Groups H and C under identical temperature and MC conditions (P > 0.05). However, the moisture absorption temperature had a significant effect on elastic swelling strain, with the strain being more pronounced at 90 °C.

In Figure 6c, viscoelastic swelling creep strain trends of both groups mirror those of elastic swelling strain, with compressive stress in surface layers and tensile stress in

**Table 3:** Parameters for the fitting equation of swelling ratio in the tangential (T) and radial (R) directions of Group H and Group C wood at temperatures of 50 °C, 70 °C, and 90 °C.

Temperature (°C)	50				70				90			
Specimen orientation	Н-Т	С-Т	H-R	C-R	Н-Т	С-Т	H-R	C-R	Н-Т	С-Т	H-R	C-R
Intercept	-2.74	-2.28	0.21	0.22	-2.24	0.22	0.28	0.33	-0.51	-0.86	0.70	0.52
Slope b	0.46	0.43	0.19	0.26	0.50	0.50	0.21	0.28	0.44	0.51	0.21	0.33
$R^2$	0.93	0.88	0.94	0.96	0.95	0.99	0.98	0.99	0.98	0.94	0.97	0.94

Specimen orientation: T (tangential direction), R (radial direction). For examples, H-T represents the wood from Group H (HT) measured in the tangential direction; C-R indicates the wood from Group C (CKD) measured in the radial direction.

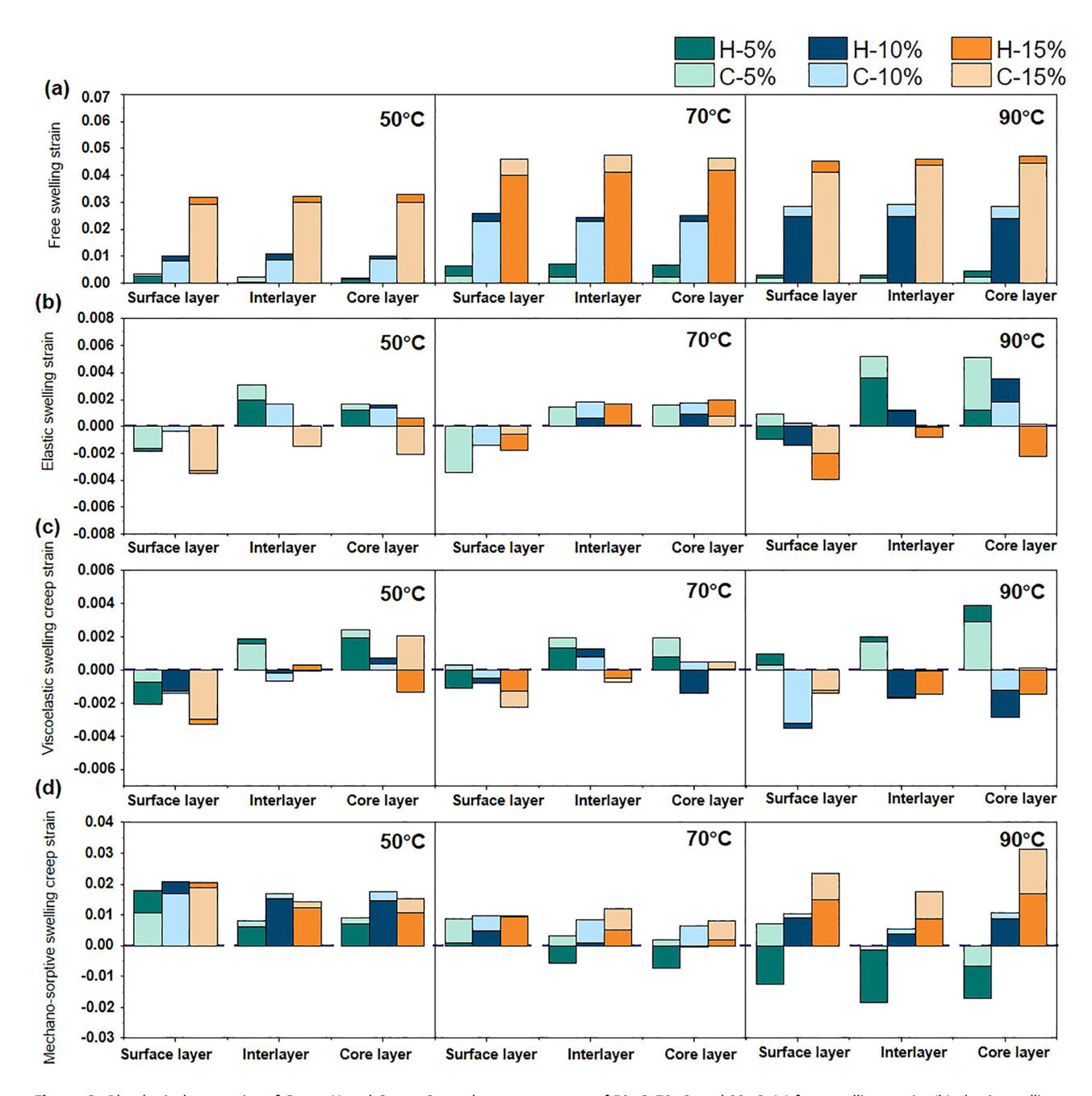


**Figure 6:** Rheological properties of Group H and Group C wood at temperatures of 50 °C, 70 °C, and 90 °C: (a) free swelling strain; (b) elastic swelling strain; (c) viscoelastic swelling creep strain; (d) mechano-sorptive swelling creep strain.

interlayers and core layer. However, compared to the elastic swelling strain, the values of viscoelastic swelling creep strain were smaller. Armstrong and Kingston (1960) reported greater creep deformation during MC decreases compared to constant MC conditions. However, in this study, despite diminishing MC gradients with increasing wood MC, compressive and tensile strains remained stable.

MSCS, representing permanent deformation from combined mechanical and moisture-induced stresses, is

more pronounced in surface layers than core layers (Figure 6d). ANOVA results indicated that MSCS differed significantly between Group H and C, with temperature strongly influencing its behavior. Except at 5 % MC, MSCS of the H group was significantly lower than that of the C group under most conditions, demonstrating that surface heat treatment effectively reduces MSCS in wood. At 70 and 90 °C, the total of the Group H was 43.7 % and 0.7 % lower than that of the Group C, respectively. At 50 °C, all layers exhibited

tensile strain during moisture absorption. As temperature rose to 70 °C and 90 °C, MSCS in Group H at 5 % MC transitioned to compressive strain, peaking at -0.184 under 90 °C conditions. However, compressive strains reverted to tensile strains as MC increased. The most abrupt MSCS changes occurred at 90 °C, underscoring temperature's critical role in governing MSCS magnitude and directionality. Consequently, the minimum MSCS observed at 70 °C, along with balanced absorption efficiency, indicated that this temperature might reduce the risks of irreversible deformation during the humidification of HT wood.

#### 4 Conclusions

- Heat treatment significantly reduced the absorptive moisture content of North American alder wood, particularly at lower temperatures. This led to less variability in MC and internal stress, which is crucial for steam-bent components as stress anisotropy can cause warping. At 50 °C, when the MC reached 10 %, the difference was the largest, at 1.54 %-points.
- Heat treatment notably reduced North American alder wood swelling, especially radially. At 90 °C, it showed a 0.89 %-point greater decrease than Group C, minimizing internal stress and strain during moisture absorption.
- During moisture absorption, differential swelling between the surface and core zones of wood induced stress, resulting in various swelling strains ( $\varepsilon_{\rm E}$ ,  $\varepsilon_{\rm V}$ ,  $\varepsilon_{\rm M}$ ) in the wood. These strains exhibited a trend opposite to that of the drying stress.
- Heat treatment notably reduced MSCS in North American alder wood. Group H had much lower values in most cases (47.3 % lower at 70 °C, 0.7 % at 90 °C). At 90 °C, MSCS showed temperature-dependent compressive -tensile transitions with the greatest changes. However, elastic and viscoelastic swelling strains in Group C and group H were similar and not significantly affected by heat treatment.

**Research ethics:** Not applicable. Informed consent: Not applicable.

Author contributions: Conceptualization, H.L.; investigation, H.L.; resources, N.H.; writing-original draft preparation J.W. N.H.; writing-review and editing, H.L.; project administration, H.L.; funding acquisition, H.L. All authors have accepted responsibility for the entire content of this manuscript and approved its submission.

Use of Large Language Models, AI and Machine Learning **Tools:** None declared.

**Conflict of interest:** The authors state no conflict of interest. **Research funding:** This work was supported by the Postgraduate Research & Practice Innovation Program of Jiangsu Province (KYCX25 1484) and National Natural Science Foundation of China under Grant (NO. 31870545, 31570558). Data availability: Not applicable.

#### References

- Armstrong, L.D. and Kingston, R.S. (1960). Effect of moisture changes on creep in wood. Nature 185: 862-863.
- Chávez, C.A., Moraga, N.O., Salinas, C.H., Cabrales, R.C., and Ananías, R.A. (2021). Modeling unsteady heat and mass transfer with prediction of mechanical stresses in wood drying. Int. Commun. Heat Mass Tran. 123:
- Ding, T., Gu, L., and Cai, J. (2015). The influence of heat treatment on the hygroscopicity and dimensional stability of wood. J. Nanjing For. Univ. 39: 143-147.
- Ermeydan, M., Babacan, M., and Tomak, E. (2021). Poly grafting into Scots pine wood: improvement on the dimensional stability, weathering, and decay resistance. Cellulose 28: 5827-5841.
- Fan, M., Ni, O., Yu, Z., Zhang, K., and Lyu, Z. (2014). Effects of heat treatment on the physical and mechanical properties of Dalbergia melanoxylon. J. Nanjing For. Univ. (Nat. Sci. Ed.) 38: 31–35.
- Feng, D. and Zhao, J. (2011). Study on the hygroscopicity and dimensional stability of heat-treated wood. J. Northwest For. Univ. 26: 200-202.
- Feng, X., Chen, J., Yu, S., Wu, Z., and Huang, Q. (2022). Mild hydrothermal modification of beech wood (Zelkova schneideriana Hand-Mzt): its physical, structural, and mechanical properties. Eur. J. Wood Wood Prod. 80: 933-945.
- Fu, Z., Zhao, J., Yang, Y., and Cai, Y. (2016). Variation of drying strains between tangential and radial directions in Asian White Birch. Forests
- Gao, X. (2016). Research on the tangential stress fatigue of wood under humidity cycling, Master thesis. Harbin Institute of Technology.
- He, Z., Qu, L., Wang, Z., Qian, J., and Yi, S. (2019). Effects of zinc chloride-silicone oil treatment on wood dimensional stability, chemical components, thermal decomposition and its mechanism. Sci. Rep. 9: 1601.
- Hill, C., Altgen, M., and Rautkari, L. (2021). Thermal modification of wood A review: chemical changes and hygroscopicity. J. Mater. Sci. 56: 6581-6614.
- Huang, N., Tang, B., Wan, C., Guo, X., and Liu, H. (2024). Differences in hygroscopicity and viscoelastic properties between heat-treated wood and conventional kiln-dried wood. J. Northeast For. Univ. 52: 97-105.
- Jiang, J. and Lyu, J. (2012). A review on the influence of high-temperature heat treatment on wood color change. World For. Res. 25: 40-43.
- Jiang, J., Du, J., Xu, X., and Mei, C. (2023). Research progress on property improvement and process optimization of thermally treated wood. Compos. Mater.: 1-16.
- Kocaefe, D., Huang, X., and Kocaefe, Y. (2015). Dimensional stabilization of wood. Current For. Reports 1: 151-161.
- Kubovský, I., Kačíková, D., and Kačík, F. (2020). Structural changes of oak wood main components caused by thermal modification. Polymers 12: 485.
- Lazarescu, C., Panagiotidis, K., and Avramidis, S. (2014). Color variation of stained wood products in association to near infrared spectroscopy scans. Eur. J. Wood Prod. 72: 81-85.

- Li, Y., Sun, H., Bao, B., Tang, R., and Pan, Y. (2008). Research progress and prospect of domestic and foreign wood heat treatment technology. Zhejiang Forestry Sci. Technol.: 75-79.
- Liu, Q., Lyu, W., Shi, Y., and Du, H. (2021). Preparation and properties of composite silicon modified heat-treated poplar wood. J. Beijing For. Univ. 43: 136-143.
- Lyu, J., Tu, D., Hu, C., Wang, X., Wang, Q., and Zhou, Q. (2023). Measurement of wood moisture content distribution by X-ray method based on control volume shrinkage model. Scientia Silvae Sinicae 59: 76-84.
- Militz, H. and Altgen, M. (2014). Processes and properties of thermally modified wood manufactured in Europe. In: Deterioration and protection of sustainable biomaterials, 1158. American Chemical Society, Washington, DC, pp. 269-285.
- Patcharawijit, A., Choodum, N., and Yamsaengsung, R. (2018). Effects of superheated steam treatment on moisture adsorption and mechanical properties of pre-dried rubberwood. Drying Technol. 37: 1647-1655.
- Rice, R.W. and Youngs, R.L. (1990). The mechanism and development of creep during drying of red oak. Holz als Roh-und Werkstoff 48: 73-79.
- Schneider, A. and Rusche, H. (1973). Sorptionsverhalten von Buchen- und Fichtenholz nach Wärmeeinwirkung in Luft und im Vakuum. Holz als Roh-und Werkstoff 31: 313-319.
- Xu, F., Li, M., Xia, J., Xu, L., Ding, H., and Li, S. (2022a). Preparation and properties of lignin-free wood/poly (methyl methacrylate) composite materials. Linchan Huaxue Yu Gongye 42: 17-23.
- Xu, K., Gao, Y., Zhang, X., Li, Z., Song, S., Wu, Y., Li, X., and Lu, J. (2022b). Effects of drying temperature on hygroscopicity and mechanical performance of resin-impregnated wood. Drying Technol. 40: 2414-2426.
- Yang, L. and Jin, H. (2021). Effect of heat treatment on the physic-mechanical characteristics of Eucalyptus urophylla S.T. Blake. Materials (Basel) 14: 6643.

- Yang, L. and Liu, H. (2020). Effect of a combination of moderatetemperature heat treatment and subsequent wax impregnation on wood hygroscopicity, dimensional stability, and mechanical properties. Forests 11: 920.
- Yang, L. and Liu, H. (2021). Study of the collapse and recovery of Eucalyptus urophydis during conventional kiln drying. Eur. J. Wood Wood Prod. 79:
- Yang, T., Wang, J., Xu, J., Ma, E., and Cao, J. (2019). Hygroscopicity and dimensional stability of *Populus euramericana* Cv. modified by furfurylation combined with low hemicellulose pretreatment. J. Mater. Sci. 54: 13445-13456.
- Yang, L., Zheng, J., and Huang, N. (2022). The characteristics of moisture and shrinkage of Eucalyptus urophylla × E. grandis wood during conventional drying. Materials 15: 3386.
- Yin, F., Ou, Y., Jiang, J., Li, Z., and Lyu, J. (2023). Research development of shrinkage and swelling of wood with multi-scale structures. Scientia Silvae Sinicae 59: 145-154.
- Yue, K., Cheng, X., Wang, L., Lu, W., Wan, L., Liu, W., and Jia, C. (2016). Effects of modification treatment on the mechanical and combustion properties of poplar wood. Combust. Sci. Technol. 22: 426-432.
- Zhang, J., Yang, L., and Liu, H. (2021). Green and efficient processing of wood with supercritical CO<sub>2</sub>: a review. Appl. Sci. 11: 3929.
- Zhong, X., Zhang, S., and Mal, N. (2021). Changes in wood cell wall pore size distribution under different moisture content states. J. Beijing For. Univ. 43: 128-136.
- Zhou, Y., Jiang, X., and Liu, J. (2006). Research and application progress of wood ultra-high temperature heat treatment technology. Wood Ind.: 1-3.
- Zhu, J. and Yang, L. (2025). Progress in the study of dry shrinkage deformation and drying stress of raw bamboo. BioResources 20: 2304-2320.